FACULTAD DE CIENCIAS DEL MAR

UNIVERSIDAD DE LAS PALMAS DE GRAN CANARIA

ATMOSPHERIC FLUXES OF SOLUBLE MAJOR IONS: TWO YEARS OF WET AND DRY DEPOSITION MEASUREMENTS AT GRAN CANARIA, SPAIN.

Xabier Aranburu Barrio

Curso 2019/2020

Dra. María Dolores Gelado Caballero

Trabajo Fin de Título para la obtención del título: Grado en Ciencias del Mar

CONTENT

1. Introduction

Transport and deposition of atmospheric particles notably affects the climate (Buseck & Pósfai, 1999; Ramanathan et al., 2001), as well as human health (Kelly & Fussell, 2015), and is considered one of the most important sources of nutrients in the oceans (Baker et al., 2006), especially in the "Low-Nutrient Low-Chlorophyll" (LNLC) zones (Jickells & Moore, 2015).

Formation of atmospheric aerosol can be the result of the transformation from gas to particle, induced by natural or anthropogenic precursors, or it can be the result of the action of the wind on both water or land (Seinfeld and Pandis, 1998). It is estimated that dust contributions to the oceans are around 450 Tg $year^{-1}$, of which about 43% are deposited on the Atlantic Ocean (Jickells et al., 2005).

Located near the African continent within the "Dust Belt" (Prospero & Lamb, 2003) the Canary Islands are frequently subjected to Saharan dust events. North Africa is the most active and wide region of dust emission, contributing 50-70% of global emissions (Huneeus et al., 2011), therefore the Canary Islands are an ideal place to study the impact of African dust episodes in the subtropical zone of the North Atlantic Ocean (NAO) (Gelado-Caballero et al., 1996; Neuer et al., 2004; Torres-Padrón et al., 2002). Dust sources on the African continent are mostly located in low-lying areas (Prospero et al., 2002), which are associated with drainage areas of ancient waterways, where river sediments accumulated during the so-called African wet periods (Middleton et al., 2018; Pausata et al., 2020; Skonieczny et al., 2015). These potential source areas, cover a large part of the Sahara, and a portion of Sahel region (Rodríguez et al., 2015; Rodríguez et al., 2020).

Spatial and seasonal variations are shown in numerous studies regarding Saharan dust transport mechanisms (Goudie & Middleton, 2001; Prospero, 1999). Air plumes that reach the Canary Islands loaded with dust are known as the "Saharan Air Layer" (SAL), a dry, warm and dust-laden corridor that expands from the North African coast (1-5 km a.s.l.) to the American continent above the marine boundary layer. During the westward movement of the SAL, and because of (size dependent) gravitational settling, dust particles move downward from the warm and dry SAL to the cooler and humid Marine Boundary Layer (MLB). Dust transport over the islands is strongly affected by the seasonal latitudinal variation of the "Intertropical Convergence Zone" (ITCZ). During the boreal summer, the ITCZ moves northward over the north western African continent, creating a thermal low over the surface of the African continent. This causes the high-

pressure system of North Africa (NA) to be located at higher altitudes likewise causing the transport of dust to rise. The emerging dust from the African coast follows the path of tropical waves, or also called eastern waves, reaching the islands from the S-SW (Sancho et al., 1992). In winter, the ITCZ is located at lower latitudes, and the transport of dust is controlled by the high-pressure systems of the north of the African continent. Dust reaches the archipelago from the east at relatively low altitudes, where it is mostly injected into the MBL (Díaz et al., 2006).

The MBL is restricted by the base of the thermal inversion layer at an altitude of about 500 m above sea level in the areas contiguous to Azores anticyclone, and at about 2000 m in the trade wind area, closer to the tropics. In the subtropical zone, the top of the MBL is usually contained by the Trade Wind Inversion Layer (TWI). In Canary Islands, the TWI`s position follows a seasonal pattern. During summer it is located at heights between 700 and 1380 m with an average thickness of 560 m, while during winter the heights rise to about 1360 and 1850 m, and the average thickness decreases to about 360m (Torres et al., 2001). During summer, African dust is transported at higher altitudes, often above the TWI, it is for this reason that TWI is believed to have a great impact on vertical deposition and therefore on the amount of dust that achieves to reach the MLB (Alonso-Pérez et al., 2007; S. Rodríguez et al., 2015; Sergio Rodríguez et al., 2020).

Atmospheric aerosol is deposited on terrestrial and marine ecosystems, either by dry deposition (DD) or Wet Deposition (WD). Different authors have studied the fluxes of particle deposition in Gran Canaria, Canary Islands, at the Tafira (TF) and Pico de la Gorra (PG) stations located at altitudes of 269 m a.s.l and 1930 m a.s.l, respectively (Menéndez et al., 2007, 2009; Gelado-Caballero et al., 2012; López-García et al., 2013). They have claimed that the DD dominates the deposition fluxes over the WD (more than 93% of total flux) with a mean value of 25.0 ± 0.3 mg m^{-2} d^{-1} for DD (López-García et al., 2013). No clear seasonality for the total deposition fluxes in the TF station has been found although intense dust events were detected during winter and early spring (December-March) seasons. However, in the PG station the mean concentration of Total Suspended Particles (TPS) increases during summer (July-September) due to the transport of dust layer occurs in higher altitude of the atmosphere.

A combination of multivariate statistical methods and backward trajectories have been used to evaluate the aerosol sources and the influence of the seasons on the TPS concentrations. For example, using chemical analysis of atmospheric deposition and Principal Component Analysis (PCA) the contribution of different sources of dust and the seasonality in the Mediterranean region have been determined (Chabbi et al., 2020;

Morselli et al., 2008). Depending on the origin of air masses, the study of the back trajectories (see for example Morselli et al., 2008; Astitha et al., 2010) allows the determination and dating of long-range dust and chemical elements . Astitha, et al. (2010) explores the origin and fate of continental aerosols transported over the Central Atlantic Ocean, in terms of chemical composition, number and size distribution, using chemistry-transport models, satellite data and in situ measurements. They observed that urban areas were subjected to high concentrations of anthropogenic pollutants, especially due to transportation and industry, which were characterized by a high concentration of ions such as NO_3^- and SO_4^{2-} amongst others. On the other hand, the marine contributions were characterized by a high concentration of Na^+ and Cl^- ions transported by the sea spray, while the presence of dust intrusions from the Sahara resulted in greater inputs of Ca^{2+} and PO_4^{3-} ions.

This work aims to study the characterization of the soluble elements of atmospheric dust depositions: the major ions (F^-, Cl^-, Br^-, NO_3^-, SO_4^{2-}, nss-SO_4^{2-}, PO_4^{3-}, Na^+, NH_4^+, K^+, Mg^{2+}, Ca^{2+}) and three organic acids (Acetic, Oxalic and Formic) and the seasonal variability of deposition fluxes on the island of Gran Canaria during a period from January 2018 to March 2020. The potential sources of the chemical species will be also established using a multivariate statistical method, the Principal Component Analysis (PCA).

2. Methodology

2.1 Sampling sites and aerosol collection

Deposition samples were collected at Tafira (TF) station (28º 06' N, 15º 24' W; 269 m ASL), located within a semi urban area and confined to the marine boundary layer (<1800 m ASL). This site was used in this and previous studies to investigate variations of the chemical signature of aerosols reaching the Canary Islands (Gelado-Caballero et al., 2012; López-García et al., 2013). A total suspended particles (TSP) concentration time-series has been recorded since1st December 2003 (Gelado-Caballero et al., 2012; López-García et al., 2013).

Samples were collected using an automatic wet and dry sampler (ARS 1000, MTX Italy) fitted with two cylindrical buckets, one is for collecting WD and the other for DD. The humidity sensor allows the DD to be isolated from the environment as soon as it starts raining. The WD bucket remains covered in absence of precipitation but when it starts to rain the humidity sensor detects it and the apparatus immediately covers the DD bucket, leaving the WD bucket free to collect the particles that are dragged in during the precipitation. DD buckets are changed every 15 days in normal conditions, while the

collection and chemical analysis of the WD is carried out immediately, as far as possible, and exchanged for a clean one. The aerosols collected in the deposition samples were quantified by gravimetry after filtering. Nucleopore filters were dried under a Class 100 horizontal laminar flow bench and weighted with an accuracy of ±0.01 mg (Sartorius CP225D), before washing with 0.1 M hydrochloric acid (Suprapure, Merck) prior to use. In this work soluble fractions from depositions collected between January 2018 and February 2020 were chemically characterised.

2.2 Chemical analysis

Soluble major ions and pH measurements were determined in the deposition samples collected. For DD samples, 150 ml of Milli-Q water was added to the bucket to wash all the particles deposited on the walls and the pH of the solution was measured. After that, the solution was filtered using an acid clean Nucleopore filter (47mm diameter and 0.2 µm pore size). WD samples were analysed just after the rain event and the same type of filtering assembly was used. The pH of unfiltered samples of dry and wet depositions were determined using a combined electrode (Aquatrode Plus, Metrohm).

Chemical composition of the water soluble fraction was measured using two ion chromatographers (883 Basic IC Plus, Metrohm), a Metrosep A Supp 4 column for anion separation (fluoride, formate, chloride, bromide, nitrate, phosphate, sulphate, acetate, and oxalate) and a Metrosep C4 column for cation separation (sodium, ammonium, potassium, calcium and magnesium) with a detection limit of 1 µg L^{-1}.

For the anion eluent, a 3.6 mM carbonate solution prepared from sodium carbonate (Fluka) was used, while for the cation eluent, a 3.5 mM HNO_3 solution was prepared from 69% nitric acid (Hiperpur grade, Panreac). In order to maintain the baseline, a 100 mM sulphuric acid solution diluted from 95-97% sulphuric acid (Suprapur grade, Sigma-Aldrich) was used as an ion suppressor. Every 4 days eluent and ion suppressor solutions were prepared. External calibration was used to determine ion concentrations. All stock calibration standards contained a concentration of 1 mg/L and were supplied by Fluka.
A Chromafil CA45-25 pre-filter was used to prevent any particles from entering the apparatus. All samples were measured twice, and the concentration of each sample has been calculated as the mean of the two replicate measurements, with the blank value subtracted.

2.3 Air mass identification

The origin of the air masses contributing to each sample was interpreted using 5-day isentropic back trajectories (finishing at altitudes of 300, 700, 1500 m in 6 hour steps) calculated for twice a day (00:00 and 12:00 UTC) using the HYSPLIT (Hybrid Single-Particle Lagrangian Integrated Trajectory) model (Rolph et al., 2017; Stein et al., 2015). We have considered 4 geographic sectors depending on source region and mineralogy: North African (Sahara), Sahelian, Marine (maritime aerosols, with trajectories over the North Atlantic Ocean), and Marine-European (Maritime aerosols, with trajectories over both North Atlantic Ocean and European continent).

3. Results

3.1 Climatic characteristics of the sampling period

The chemical composition of aerosol particles varies widely as to the content of the mineral, marine, or anthropogenic compounds result from the relative contribution of each aerosol source sectors. In this work, two primary sources have been classified: African and non-African sources. The air masses coming from the African continent correspond with the arid areas of the Sahara Desert, North Africa (NA) and Sahel (NA-SHA). Air masses coming from marine sectors, are divided into Marine-European trajectories (NAO-EU), and those coming only from the marine sector (NAO) as shown in Figure 1.

HYSPLIT back trajectories have been analysed between January 2018 and March 2020 to determine the origin of the particles collected during the period of days in which 37 samples of DD (25) and WD (12) were taken (see Figure 2). During this period, similarities were found in frequency and seasonality in relation to previous years (Maria D. Gelado, personal communication, September 9, 2020) and the amount of rainfall measured during the sampling period is within the mean values when compared with the 15-year time series measured in TF station (see supplementary material, Figures S1 and S2). Air masses from the Sahara Desert were predominant during winter, while spring was the scarcest season. A slight increase in air masses from Sahel Desert was detected in summer along with a more accentuated increase in marine air masses during spring and summer. Marine-European air masses predominate in summer.

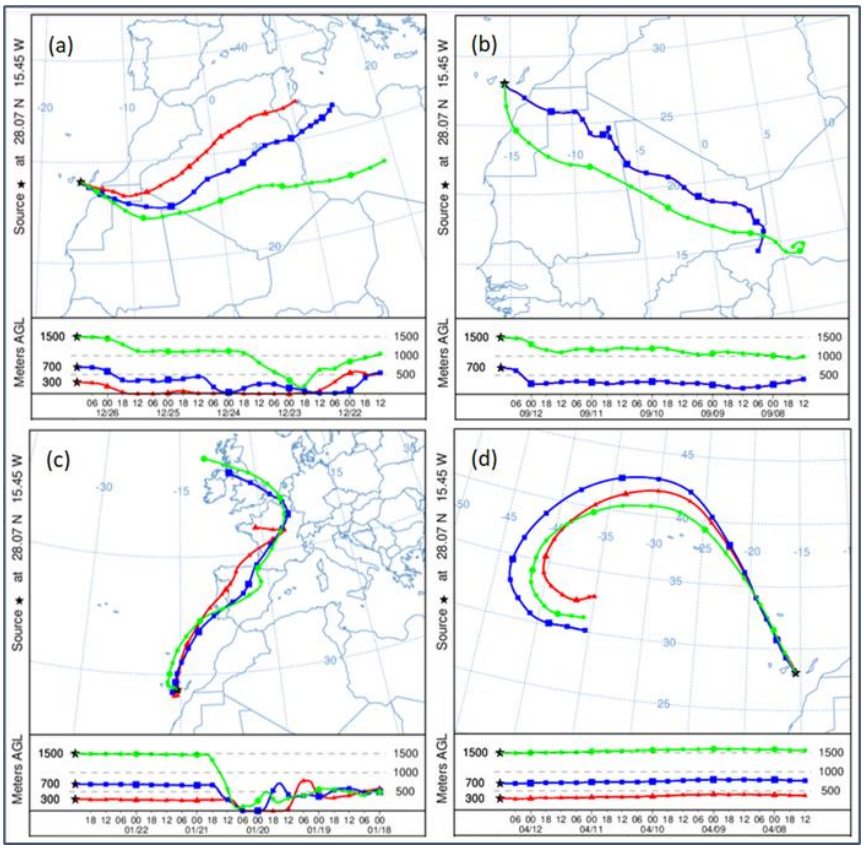

Figure 1: Classification of the different back-trajectories of air masses with end point in Gran Canaria. Geographical sectors: (a) NA (North Africa 20°N-30°N, 18°W-15°E), (b) NA-SHA (Sahel 10°N-20°N, 18°W-15°E), (c) NAO-EU (trajectories over the North Atlantic Ocean, Europe or both), (d) NAO (North Atlantic Ocean).

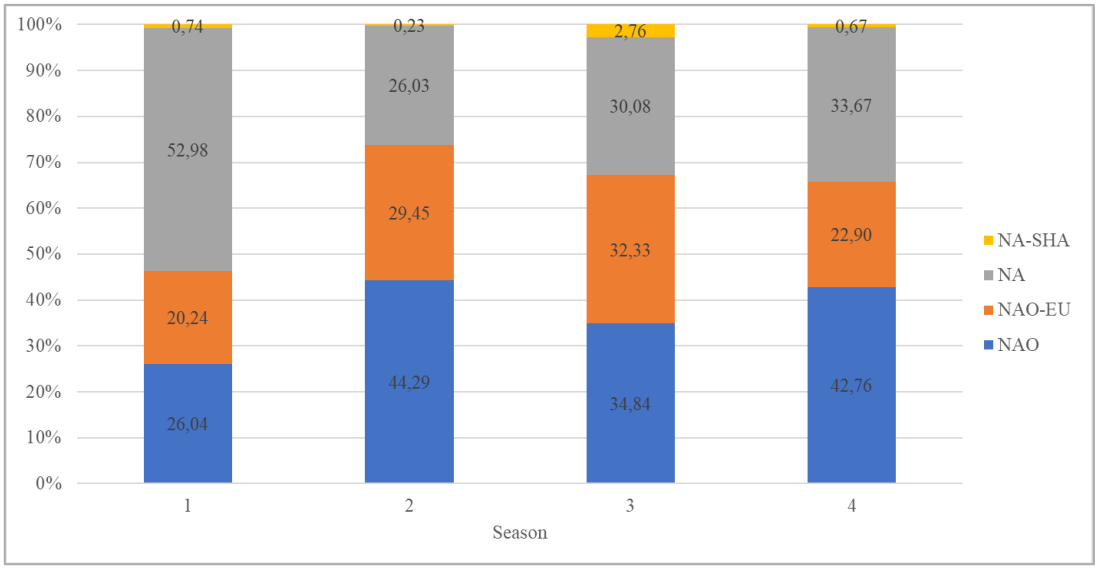

Figure 2: Air mass classification using HYSPLIT model for the period January 2018 to March 2020. Four origins were used: NA-SHA, North Africa-Sahel; NA, North Africa; NAO-EU, North Atlantic Ocean-Europe; NAO, North Atlantic Ocean. 1, Winter; 2, Spring; 3, Summer; 4, Autumn.

3.2 Seasonality of deposition fluxes

Figure 3 shows values of TPS concentrations measured in TF and PG stations from January 2018 to March 2020. Average TSP concentrations during this period was 28.82 ± 51.89 μg m^{-3} (21.06 μg m^{-3} geometric mean) with a minimum of 2.00 μg m^{-3} and a maximum of 960.70 μg m^{-3}.

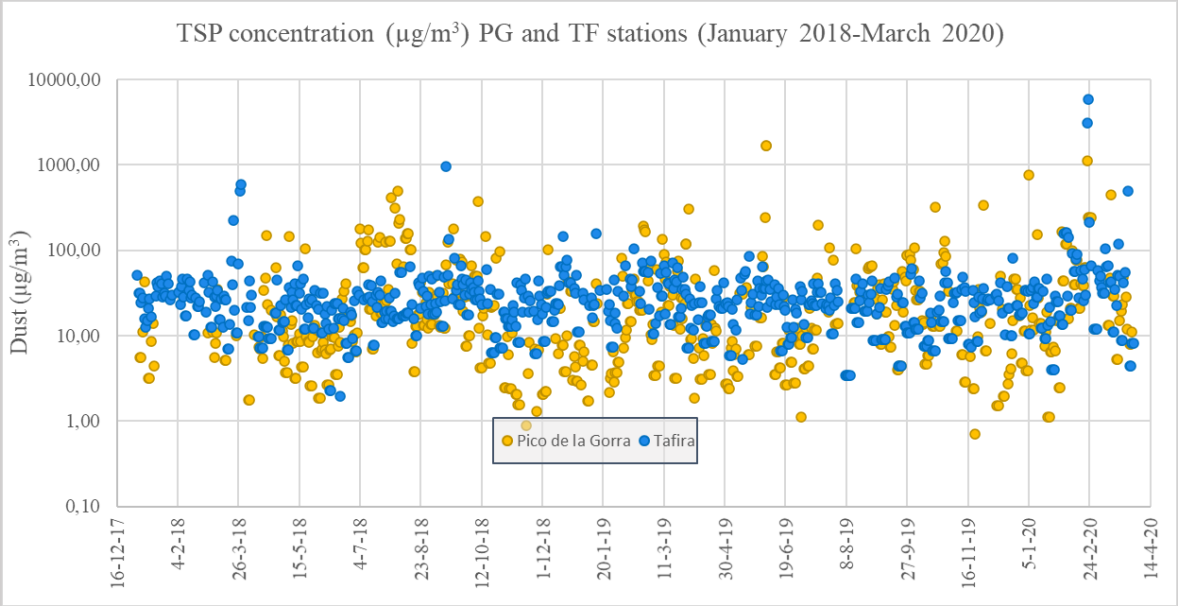

Figure 3: TSP concentrations (μg/m^3) for PG and TF stations for the period January 2018 to March 2020.

Figure 4 shows the particle deposition fluxes for wet and dry deposition samples. The average of particle deposition fluxes in the dry mode was 24.60 ± 5.60 mg m^{-2} d^{-1} while for the wet mode was 12.29 ± 7.34 mg m^{-2} d^{-1} for days with rainfall. WD corresponds to 1.4% of the total particle flux collected during the studied period.

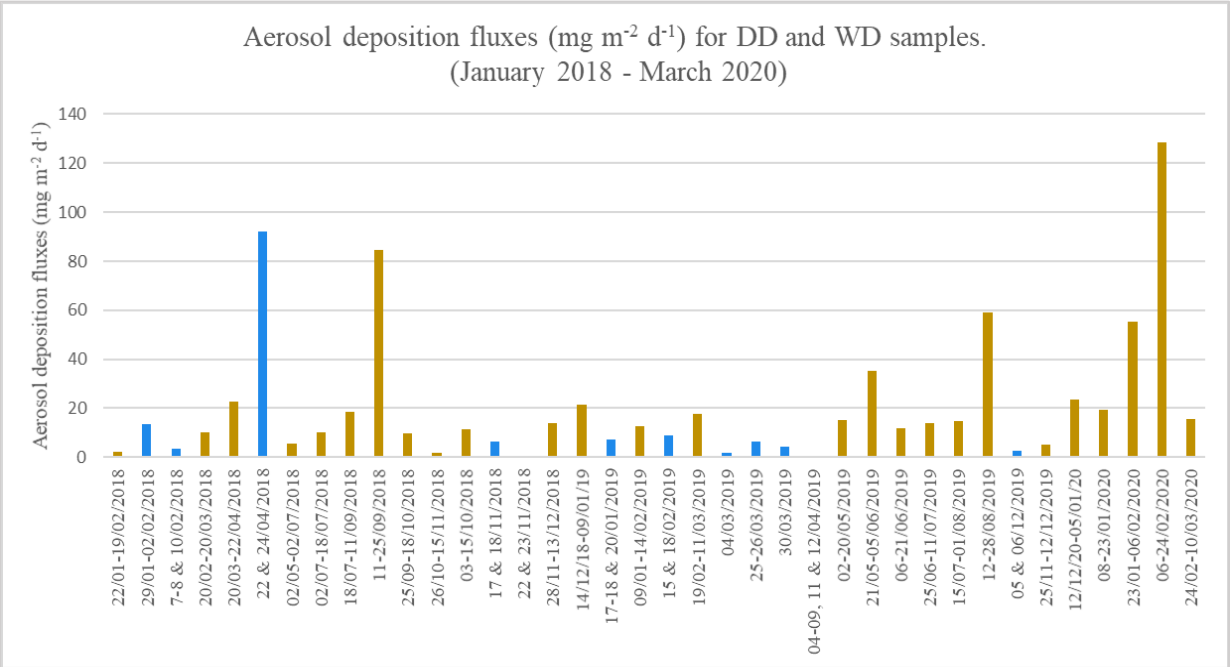

Figure 4: Aerosol deposition fluxes (mg m^{-2} d^{-1}) For DD (brown) and WD (blue) samples for the period January 2018 to March 2020.

In Figures 5 and 6 seasonal particle deposition fluxes are shown for DD and WD samples, respectively. With respect to the particle deposition fluxes for DD, it was observed that the highest average fluxes value as well as the most intense events predominated in winter and summer. Spring showed slightly lower values than previously mentioned seasons and no major dust events occurred during this period. Autumn on the other hand, was clearly the season with the least contribution of dust without any significant dust event.

Regarding WD fluxes, it was observed that the highest mean value corresponded to the winter for DD samples, even though any major dust event did not occur during this season. Summer showed slightly lower mean values than winter, although a major Saharan dust event could be observed. Autumn on the other hand, is clearly the season with the least contribution of dust resulting in a DD flux close to the background levels of the TF station (9.07 mg m^{-2} d^{-1}). There was no rainfall during the summer season.

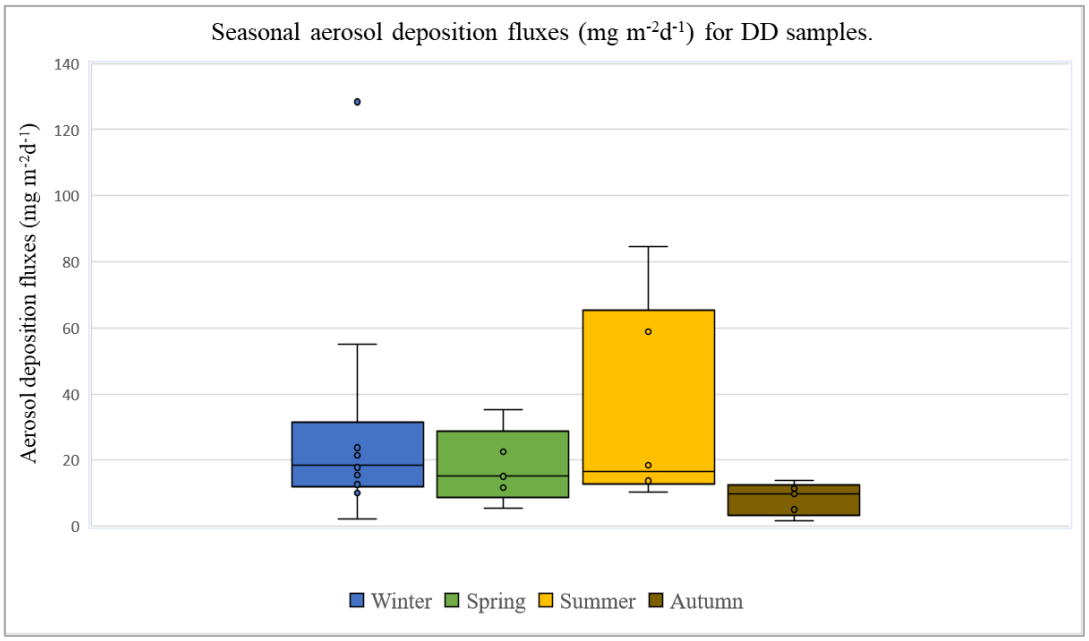

Figure 5: Particle deposition fluxes for DD (mg $m^{-2}d^{-1}$) in TF station for each season. From January 2018 to March 2020.

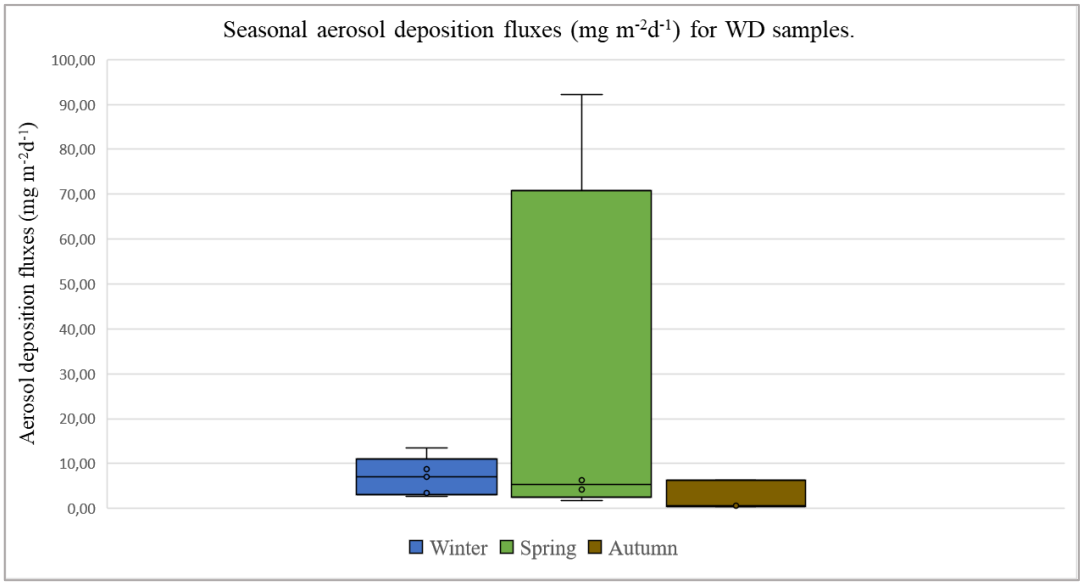

Figure 6: Particle deposition fluxes for WD (mg $m^{-2}d^{-1}$) in TF station for each season. From January 2018 to March 2020. No rainfall was measured during summer.

3.3 Characterization of soluble elements.

The pH and soluble elements of DD and WD were analysed for 38 samples. The mean pH for DD samples was 7.41 ± 0.17 (range between 5.48-9.89), whereas for the WD, the mean pH of the samples was 6.92 ± 0.20 (range between 5.70-8.03).

Average values of soluble element fluxes for DD and WD samples for the whole period are shown in the Table 1. In general, WD values showed a larger variability compared to DD, in addition, the frequency and intensity of WD events were more variable and rainfall samples presented a shorter period (mainly 2 days).

Although WD fluxes constitute a small fraction of total particle fluxes, it represents a significant input of soluble elements such as Br^- and NH_4^+ (Table S1).

	F^-	Ac	Fo	Cl^-	Br^-	NO_3^-	PO_4^{3-}	SO_4^{2-}	nss-SO_4^{2-}	Ox	Na	NH_4^+	K^+	Mg^{2+}	Ca^{2+}
DD	0,55	3,01	5,97	114,97	0,04	59,00	0,19	7,08	2,25	0,57	85,25	0,63	2,76	10,51	22,82
	(0,71)	(5,48)	(10,56)	(80,27)	(0,04)	(27,64)	(0,12)	(5,44)	(2,54)	(0,56)	(60,72)	(0,51)	(1,55)	(6,77)	(21,04)
WD	0,03	36,66	36,58	1817,36	3,02	93,14		119,96	26,06	1,35	1480,26	108,62	34,58	170,48	119,37
	(0,02)	(62,00)	(57,24)	(1217,55)	(1,22)	(89,77)		(58,35)	(26,41)	(0,79)	(1102,47)	(77,60)	(23,82)	(119,38)	(59,77)

Table1. Average of fluxes of soluble elements (µmol m-2 d-1) and standard deviation (in brackets) from January 2018 to March 2020 for DD and WD samples. Values for WD represent only the average for raining days. Acid acetic (Ac), Formic (Fo) and Oxalic (Ox).

3.4 Principal Component Analysis

Common factors influencing the elemental composition were investigated using the principal component analysis (PCA) method with Varimax rotation and the SPSS statistical software package. Table 2 the Varimax rotated component matrix and shows the possible main aerosol sources of these ions for DD and WD samples. The PCA analysis of the dry depositions fluxes presented three main components (PCs) which explain 88.41% of the variance, while three PCs were obtained for the analysis of the wet deposition which explain 93.5% of the variance.

The PCA analysis for DD samples (Table 2) reveals that the solubility of each ion depends on its source. One of the PCs accounts for 42.14% of the variance and ions that are strongly correlated with mineral aerosols are shown (Ca^{2+}, PO_4^{3-}, nss-SO_4^{2-} and F^-), along with the organic acid anions Acetate (Ac), Formate (Fo) and Oxalate (Ox). A second group shows ions that are strongly correlated with marine aerosols (Na^+, Cl^-, K^+, Mg^{2+}, Br^- and SO_4^{2-}), and the third group only includes ion NH_4^+ which could be of anthropogenic origin. The ion NO_3^- presents similar correlations in the marine and mineral PCs.

On the other hand, in the PCA for WD three main PCs are distinguished. The first component (Table 2) accounts for 51.28% of the variance and the ions (Na^+, Cl^-, K^+, Mg^{2+}, Br^- and SO_4^{2-}) are strongly correlated with marine aerosols. The second component contains NO_3^- and nss-SO_4^{2-} ions, indicating that this component could be related with both anthropogenic and mineral sources. The third component comprises the organic acid anions Acetate (Ac) and Formate (Fo). The Ca^{2+} ions are divided with similar weights between the first (marine) and second component (crustal). Similarly, the NH_4^+ ions are equally correlated well with both the second and third groups.

	Component					
	Marine		**Crustal**		**Chemical aging**	**Anthropogenic**
Fluxes (nmol m-2 d-1)	**DD**	**WD**	**DD**	**WD**	**WD**	**DD**
F^-			0.894			
Cl^-	0.969	0.992				
Br^-	0.725	0.755				
NO_3^-	0.602		0.605	0.964		
SO_4^{2-}	0.757	0.936				
$nss\text{-}SO_4^{2-}$			0.855	0.799		
PO_4^{3-}			0.798			
CH_3COO^-			0.922		0.961	
$CHOO^-$			0.935		0.960	
$C_2O_4^{2-}$			0.893			
Na^+	0.971	0.980				
$NH4^+$				0.667	0.592	0.935
K^+	0.896	0.974				
Mg^{2+}	0.966	0.985				
Ca^{2+}		0.703	0.922	0.679		

Table 2: Varimax rotated component matrix for DD and WD samples.

3.5 Seasonality

Seasonal changes were observed in the concentrations of individual ions that could be associated to the seasonal variability of different types of air mass (Table 3). In DD samples, the highest soluble fluxes were measured in summer, while the spring is the season with the lowest concentrations during the studied period in this work. Ammonium is the only chemical species in DD that presents a different pattern from the others.

The typical ions of mineral of dust such as Ca^{2+}, $nss\text{-}SO_4^{2-}$, F^- and oxalate follow a similar seasonal pattern, having their highest concentrations during winter and summer and the lowest fluxes during spring and autumn. On the other hand, Cl^-, NO_3^-, Na^+, K^+ and Mg^{2+} ions were mainly present in the sea spray and marine aerosols with a similar tendency in spring and autumn.

In general, seasonal WD fluxes for all water-soluble species studied were at their greatest values during winter and autumn, coinciding with periods of significant rainfall events (see supplementary materials Figure S2). Major ions characteristic of dust such as Ca^{2+} and $nss\text{-}SO_4^{2-}$ predominated in the spring fluxes whereas typical ions of marine aerosol such as Cl^-, SO_4^{2-}, Na^+, K^+ and Mg^{2+} dominated the WD during rainiest seasons of winter and autumn in the region.

Season	DD/WD	F^-	Ac	Fo	Cl^-	Br^-	NO_3^-	PO_4^{3-}	SO_4^{2-}	nss-SO_4^2	Ox	Na	NH_4^+	K^+	Mg^{2+}	Ca^{2+}
W	**DD**	0,44	1,81	4,28	76,95	0,04	43,52	0,14	5,53	2,05	0,44	60,09	0,62	2,00	7,23	19,30
		(0,61)	(1,80)	(5,02)	(41,23)	(0,02)	(13,79)	(0,06)	(2,13)	(1,49)	(0,33)	(30,05)	(0,38)	(0,71)	(3,25)	(13,61)
	WD	0,02	13,30	16,79	2455,41	2,69	53,10		142,10	15,24	1,35	2102,27	68,66	45,06	239,71	108,49
		(0,01)	(7,75)	(11,42)	(1213,59)	(1,44)	(41,36)		(67,18)	(11,13)	(0,79)	(1106,09)	(20,38)	(19,26)	(116,06)	(25,87)
Sp	**DD**	0,30	0,92	2,89	122,51	0,04	63,32	0,21	4,74	1,39	0,45	94,77	0,15	2,77	10,77	15,09
		(0,13)	(0,46)	(2,65)	(34,17)	(0,03)	(19,63)	(0,08)	(4,32)	(0,83)	(0,14)	(28,72)	(0,03)	(0,65)	(3,33)	(4,04)
	WD		22,76		604,23		193,81		85,13	53,90		351,29	154,20	8,39	47,11	146,16
			(15,71)		(53,31)		(118,58)		(33,85)	(33,15)		(103,68)	(92,66)	(1,75)	(1,85)	(109,55)
Su	**DD**	0,93	6,87	12,67	183,34	0,06	81,78	0,29	12,54	3,15	1,03	134,35	0,43	4,09	16,25	39,38
		(1,07)	(10,28)	(19,77)	(125,64)	(0,06)	(40,01)	(0,17)	(8,01)	(4,27)	(0,96)	(98,81)	(0,25)	(2,30)	(10,88)	(36,16)
	WD															
Au	**DD**	0,39	2,57	3,57	88,54	0,04	54,29	0,14	5,34	1,78	0,30	62,58	1,21	2,66	9,77	16,45
		(0,19)	(1,98)	(2,22)	(47,76)	(0,01)	(18,70)	(0,03)	(1,73)	(1,06)	(0,13)	(40,60)	(0,71)	(1,69)	(4,51)	(6,35)
	WD	0,04	89,49	76,15	1967,06	3,66	59,22		117,88	16,25		1572,55	129,65	43,30	178,48	110,71
			(114,06)	(106,26)	(1097,62)	(0,13)	(43,29)		(61,66)	(23,24)		(853,04)	(113,67)	(25,98)	(96,97)	(55,10)

Table 3. Average and standard deviation (in brackets) concentration (μmol m^{-2} d^{-1}) of soluble elements from DD and WD samples. W, winter; Sp, spring; Su, summer; Au, autumn.

4. Discussion

Comparing the HYSPLIT back trajectories that have been analysed between January 2018 and March 2020 (see Figure 1) with those reported by López-García (2020), a similar seasonality in the air masses could be observed. Figure 2 shows that air masses coming from the African continent predominate in winter followed by summer and autumn but a lower African air mass frequencies were found (53.7, 23.3, 32.8 and 34.3% for winter, spring, summer and autumn seasons, respectively) than those previously mentioned for this station (64, 43.7, 51 and 50% for winter, spring, summer and autumn seasons, respectively). This could be attributed to the higher number of back trajectories analysed (750, 1500, 2000, 2500, 3000 and 3500 m a.s.l.) including higher altitude compared to the present work (300, 700 and 1500m a.s.l.). Despite this, Figure 2 provides a representative seasonal pattern of air masses at the TF station. As many dust outbreaks reaching Canary Islands come from higher atmospheric layers, gravitational dust settling (i.e. dust particles moving downwards from the SAL) could be considered as a significant contributing factor in the seasonality of mineral dust concentration in the MBL.

Average TSP concentrations in TF station during the sampling period was 28.82 ± 51.89 μg m^3 (21.06 μg m^3 geometric mean). For previous years (2000-2019) the average TPS was 32.23 ± 41.22 μg m^3 (geometric mean 22.47 μg m^3) in the same station, very close to those measured in this work (Maria D. Gelado, personal communication, September 9, 2020).

In addition, the mean particle deposition fluxes in the dry mode was 24.6 ± 5.6 mg m^{-2} d^{-1} while for the wet mode was 12.29 ± 7.34 mg m^{-2} d^{-1} for days with rainfall. These results are in good agreement with those previously published for the period (2009-2012) at the TF station (López-García et al., 2013). Wet deposition fluxes account the 1.4% of the total (wet and dry) flux, which is a slightly lower value that is given for the mentioned period 2009-2012.

Seasonal changes were observed in the concentrations of deposition fluxes that could be mainly associated to the seasonal variability of different types of air masses. In Figures 5 and 6, the particle deposition fluxes are shown for DD and WD samples, respectively.

In the case of the dry mode deposition, it is observed that the highest mean particle fluxes value occur in winter (30.6 mg m^{2-} d^{-1}) when the most intense dust events take place since TWI is located at higher altitudes and the dust reaches the archipelago at relatively low altitudes where it is mostly injected into the MBL. This is also observed in the results of

Figure 3, where high concentrations of TPS are observed during winter in the lowest altitude layers (TF: 269 m a.s.l.) while in higher air mass layers (PG: 1900m a.s.l.), relatively low concentrations are shown. During summer, the TWI it is located at lower altitudes and dust reaches the archipelago at higher altitudes, therefore the TWI can act as a dust barrier preventing dust precipitation to the MLB (see Figure 3). Even so, relatively high average concentrations of deposition fluxes and an important dust outbreak were measured during summer (29.4 mg m^{-2} d^{-1}). During the spring slightly lower values than the previously mentioned seasons and no major dust events occurred. These results obtained are in good agreement with those obtained for long term aerosol measurements in Gran Canaria in the PG station (Gelado-Caballero et al., 2012).

Regarding WD fluxes, the highest average of fluxes value corresponds to winter and lower values correspond to autumn as the seasonal trend observed in the DD.

The mean pH value was 7.41 ± 0.17 in the DD and 6.92 ± 0.20 in the WD samples. The higher pH values (up to 9.89) in the DD samples occur when largest African dust concentrations are presented (R^2: 0.8). Similarly, in WD samples, the pH increases (up to 8.03) with the rise of dust concentration during the African dust outbreaks (R^2: 0.57). This was expected since mineral dust aerosols are considered alkaline due to its high proportion of calcareous components that could neutralize the acidic compounds present in the atmospheric aerosols increasing the rain pH (pH > 5.6) (see Avila et al., 1998).

The DD and WD fluxes of soluble major ions for the whole period (Table 1) show a larger variability of WD compared to DD due to scarce and irregular rainfall events. DW samples last for less than 3 days on average while the sampling period for DD samples was around 20 days long. Thus, DD measurements smooth the inputs of the sporadic African dust events over the whole sampling period. However, the WD measurements are strongly dependent on the frequency and intensity of rainfall events and the African dust concentration in the previous days.

Although WD fluxes constitute a small fraction of total particle fluxes (1,4%), it represents a significant input of soluble elements such as SO_4^{2-}, Ca^{2+} or Cl^- (28.63, 12.11 and 30.25% respectively). Various previous studies have noted the importance of scavenging (wash-out) in determining the final chemical composition of rainwater (Desboeufs et al., 2010). The low pH of the rain could increase the input of dissolved inorganic elements such as phosphates and iron to the surface waters from the dust having a significant effect in the ocean biogeochemistry (Korte et al., 2018; Ridame et al., 2014).

Due to the low number of WD samples where concentration of oxalate, F^- and PO_4^{3-} were greater than the detection limit, fluxes of these elements have not been included in the WD PCA. Overall, the two PCA analyses show four main groups: marine, crustal, chemical aging and anthropogenic.

In the marine group component, major ions such as (Na^+, Cl^-, K^+, Mg^{2+} and Br^-) are shown strongly correlated. The Na/Cl ratio (by weight) for DD and WD samples is 0.56, indicating that there is not a significant deficit of Cl^- by heterogeneous reactions and that they mostly have a marine origin (Millero, 1974). The presence of an anthropogenic compound like sulphate in the marine component suggests that it has mainly a regional origin. The most important anthropogenic sources of sulphate are fossil fuel combustion for energy production, and industrial activities in big cities and their surroundings (Lee et al., 2011).

The crustal component includes Ca^{2+}, PO_4^{3-}, F^-, nss-SO_4^{2-}, NO_3^- and other species that are associated with mineral dust such as organic acids Oxalate, Formate and Acetate. Several studies indicate that Ca^{2+} is one of the most abundant components of aerosols linked to the continental erosion of carbonate rocks (López-García (2020); Gelado-Caballero et al., 2012)), although it can also be associated with marine origin as can be seen in the case of the WD samples.

PO_4^{3-} has a high correlation with Ca^{2+} (R^2: 0.75) due to the fact that phosphates in the atmosphere are also associated with mineral dust (phosphate rocks or minerals such as apatite, indeed, one of the largest deposits of apatite are located near the coasts of Western Sahara, a dust source of the outbreaks in the Canary region).

Most of the fluoride collected in the DD samples appears to come from natural sources due to the close correlation with the calcium ion (R^2: 0.82). Airborne fluoride exists in gaseous and particulate forms emitted from both natural and anthropogenic sources, for example, fluoride-containing pesticides contribute to the release of fluoride (Rodgers et al., 2002) and can be transported over large distances (Sloof et al., 1989). Unfortunately, there are not enough F^- data in the wet fraction to evaluate their potential sources.

The nss-SO_4^{2-} also shows a high correlation with soluble Ca^{2+} (R^2: 0.753). This correlation may indicate the presence of mineral gypsum (present throughout the Sahara Desert) which is formed by the reaction of SO_2 with the airborne carbonate (Desboeufs & Cautenet, 2005; Johansen et al., 2000).

In the case of NO_3^-, its well known that traffic leads to elevated concentrations of NO_3^- (Cuevas et al., 2014) and due to the location of the sampling station TF, show higher concentrations of NO_3^- than at a rural station (López-García et al., 2017), principally in filter samples with marine and European origins. Nonetheless, nitrate is just as well correlated with the crustal and anthropogenic groups in DD samples, and it is very well correlated with the crustal group in WD samples. (Deshmukh et al., 2016) proposes a hypothesis which says that the nitrate found in aerosols in India is probably due to the formation of $Ca(NO_3)_2$ after the absorption of NO_2 or aqueous HNO_3 on the dust particles; There is a good correlation between calcium and nitrate (R^2: 0.770).

Organic acids are also closely correlated to calcium (Ac./Ca^{2+} (R^2: 0.904), Fo./Ca^{2+} (R^2: 0.864), Ox./Ca^{2+} (R^2: 0.951)) so they could be associated with mineral dust. (Deshmukh et al., 2016) claimed that the water-soluble organic carbon in the coarse mode particles is the result of the adsorption of organic compounds on the surface of the dust particles.

Chemical aging components include the organic acids formate and acetate ions, whose precursors may have predominantly anthropogenic and regional origins. Formic and acetic acids have different sources like direct emissions by vegetation (Talbot et al., 1990), indirect formed via the oxidation of ethane and propene by ozone (Calvert & Stockwell, 1983), oxidation of isoprene (Andreae et al., 1987) and in the reaction of ozone with olefins (Calvert & Stockwell, 1983).

Anthropogenic ammonium emissions originate mainly from agriculture activities including soils, fertilizers and domesticated animals waste (Bouwman et al., 1997), although traffic emissions are also important sources of ammonia in urban areas (Pandolfi et al., 2012). In addition, the TF station is also close to a field where potatoes are grown, and fertilizer is applied twice per year during late spring and late autumn. This could explain the no-correlation of the ammonium with the other water-soluble ions studied (see Table 3) as the NH_4^+ concentrations could be determined by a local origin.

Fluxes of Ca^{2+}, nss-SO_4^{2-}, F^- and oxalate were at their greatest during summer for the DD samples in agreement with other measurements in the subtropical North Atlantic region (López-García (2020); (Powell et al., 2015)) and correlated with the crustal component in the PCA. These particles are probably deposited predominantly from the SAL transported in summer at higher altitudes (Prospero et al., 2014). During the sampling period no rainfall events were measured during the summers. Thus, the spring was the season with greatest mean concentrations of Ca^{2+} and nss-SO_4^{2-} for WD samples due to an important dust outbreak during this season although the rainfall events were scarce.

In conditions without important dust events ions characteristic of dust such as fluoride and oxalate could not be measured in the WD samples because they could not exceed the detection limit of the ion chromatograph, whereas in high dust conditions these elements were measurable. In example to this, in spring 2018 a WD sample was taken corresponding to 2 days of rain after a great dust outbreak (see Figure 4), and account to the 62.55% of the total fluxes measured , as well as the 92 and 88% of the total fluxes of fluoride and oxalate, respectively, showing a strong correlation of these elements to mineral dust. This is likely the reason why spring is the season with greatest concentrations of calcium, fluoride and oxalate among others.

The soluble fluxes of Cl^-, NO_3^-, Na^+, K^+ and Mg^{2+} are prevalent during the spring and autumn corresponding with the periods with a major percentage of NAO back trajectories and rainiest seasons.

In general, WD fluxes for the soluble species studied in this period (except crustal) were increased during the autumn and winter months, coinciding with periods of significant rain events (see supplementary material Figure S2). Comparing the contribution of soluble element fluxes of DD and WD samples a clear predominance of dry deposition is observed (see supplementary material Table S1). These inputs may have a significant effect in the region since the wash out of the small particles at low pH could increase the dissolution of nutrients (for example, phosphate and iron) from the aerosol deposited. This effect has been reported in seeding experiments in the North Atlantic ocean (Korte et al., 2018) which showed that the “wet” dust deposition increases the concentration of nutrients in the waters.

5. Conclusions

The Canary Islands are subject to significant dust inputs throughout the year. Dry deposition shows a strong dominance in the atmospheric delivery of deposition fluxes. The winter and summer are the seasons with the greatest dust contributions in TF station.

WD constitutes a small fraction of total particle fluxes (1.4%) but it represents an significant input of water-soluble elements when it occurs after a dust outbreak.

In this study, the main ionic soluble-water species in the wet and dry deposition collected in a semi urban site have led to a comprehensive evaluation of the different sources which contribute to the total dust flux. By using PCA for exploratory data analysis, three main

sources of aerosol particles have been identified: marine, crustal and anthropogenic origin. Depending on the deposition mode, the anthropogenic components could have local or regional perturbations. In the marine component (Na^+, Cl^-, K^+, Mg^{2+}, SO_4^{2-} and Br^-), a regional scale contribution to the SO_4^{2-} concentration could be claimed. Moreover, anthropogenic contributions to NH_4^+ concentration may be attributed to a singular local source as agriculture.

The particle chemical aging could explain the organic acids closely correlated as these species are important contributors to the particle aging chemistry of mineral dust and sea salt. To obtain a better understanding of the lifecycles of the organic acids in the Canary Islands region, it is necessary to study a wider range of these soluble organic species and to obtain longer time series of data in order to clearly establish seasonal patterns.

The chemical composition of the soluble fluxes reflected the impact of Saharan dust inputs, specially, in the WD after intense dust outbreaks. The crustal component is characterised by Ca^{2+}, PO_4^{3-}, nss-SO_4^{2-}, F^- and NO_3^- and well related with the occurrence of African air masses in the Canary Region during winter and summer. During spring and autumn, soluble fluxes of Cl^-, NO_3^-, Na^+, K^+, SO_4^{2-} and Mg^{2+} are prevalent as a consequence of a major percentage of Marine and European trajectories.

Finally, this study in particular has expanded previous knowledge regarding the chemical composition of water-soluble ionic species in wet and dry deposition fluxes in the Canary Islands Region. The field would benefit from future research that extends this understanding and analysis to trace element species such as Al, Co, Mn and Fe in the aerosols, as these are the limiting micronutrients for primary production in the oceans.

6. Acknowledgements

The authors gratefully acknowledge the NOAA Air Resources Laboratory (ARL) for the provision of the HYSPLIT transport and dispersion model and/or READY website (http://www.ready.noaa.gov) used in this publication.

7. References

Alonso-Pérez, S., Cuevas, E., Querol, X., Viana, M., & Guerra, J. C. (2007). Impact of the Saharan dust outbreaks on the ambient levels of total suspended particles (TSP) in the marine boundary layer (MBL) of the Subtropical Eastern North Atlantic Ocean. *Atmospheric Environment*, *41*(40), 9468–9480. doi: 10.1016/j.atmosenv.2007.08.049.

Andreae, M. O., Talbot, R. W., & Li, S. M. (1987). Atmospheric measurements of pyruvic and formic acid. *Journal of Geophysical Research*, *92*(D6), 6635–6641. doi: 10.1029/JD092iD06p06635.

Astitha, M., Kallos, G., Spyrou, C., O'Hirok, W., Lelieveld, J., & Denier Van Der Gon, H. A. C. (2010). Modelling the chemically aged and mixed aerosols over the eastern central Atlantic Ocean-potential impacts. *Atmospheric Chemistry and Physics*, *10*(13), 5797–5822. doi: 10.5194/acp-10-5797-2010.

Avila, A., Alarcón, M., & Queralt, I. (1998). The chemical composition of dust transported in red rains - Its contribution to the biogeochemical cycle of a Holm Oak Forest in Catalonia (Spain). *Atmospheric Environment*, *32*(2), 179–191. doi: 10.1016/S1352-2310(97)00286-0.

Baker, A. R., Jickells, T. D., Witt, M., & Linge, K. L. (2006). Trends in the solubility of iron, aluminium, manganese and phosphorus in aerosol collected over the Atlantic Ocean. *Marine Chemistry*, *98*(1), 43–58. doi: 10.1016/j.marchem.2005.06.004.

Bouwman, A. F., Lee, D. S., Asman, W. A. H., Dentener, F. J., Van Der Hoek, K. W., & Olivier, J. G. J. (1997). A global high-resolution emission inventory for ammonia. *Global Biogeochemical Cycles*, *11*(4), 561–587. doi: 10.1029/97GB02266.

Buseck, P. R., & Pósfai, M. (1999). Airborne minerals and related aerosol particles: Effects on climate and the environment. *Proceedings of the National Academy of Sciences of the United States of America*, *96*(7), 3372–3379. doi: 10.1073/pnas.96.7.3372.

Calvert, J. G., & Stockwell, W. R. (1983). Acid generation in the troposphere by gas-phase chemistry. *Environmental Science and Technology*, *17*(9), 428A-443A. doi: 10.1021/es00115a002.

Chabbi, I., Bahloul, M., Dammak, R., Baati, H., & Azri, C. (2020). Wet deposition of major ions and trace elements in rural and coastal-urban sites in Monastir Region, Eastern Tunisia. *Arabian Journal of Geosciences*, *13*(2). doi: 10.1007/s12517-019-5014-8.

Cuevas, C. A., Notario, A., Adame, J. A., Hilboll, A., Richter, A., Burrows, J. P., & Saiz-Lopez, A. (2014). Evolution of NO_2 levels in Spain from 1996 to 2012. *Scientific Reports*, *4*(1), 1–8. doi: 10.1038/srep05887.

Desboeufs, K., Journet, E., Rajot, J.-L., Chevaillier, S., Triquet, S., Formenti, P., & Zakou, A. (2010). Chemistry of rain events in West Africa: evidence of dust and biogenic influence in convective systems. *Atmospheric Chemistry and Physics*, *10*(19), 9283–9293. doi: 10.5194/acp-10-9283-2010.

Desboeufs, K. V., & Cautenet, G. (2005). Transport and mixing zone of desert dust and sulphate over Tropical Africa and the Atlantic Ocean region. *Atmospheric Chemistry and Physics Discussions*, *5*(4), 5615–5644. doi: 10.5194/acpd-5-5615-2005.

Deshmukh, D. K., Kawamura, K., & Deb, M. K. (2016). Dicarboxylic acids, ω-oxocarboxylic acids, α-dicarbonyls, WSOC, OC, EC, and inorganic ions in wintertime size-segregated aerosols from central India: Sources and formation processes. *Chemosphere*, *161*, 27–42. doi: 10.1016/j.chemosphere.2016.06.107.

Díaz, A. M., Díaz, J. P., Expósito, F. J., Hernández-Leal, P. A., Savoie, D., & Querol, X. (2006). Air masses and aerosols chemical components in the free troposphere at the subtropical Northeast Atlantic region. *Journal of Atmospheric Chemistry*, *53*(1), 63–90. doi: 10.1007/s10874-006-2644-5.

Gelado-Caballero, M. D., Torres-Padrón, M. E., Hernández-Brito, J. J., Herrera-Melián, J. A., & Pérez-Peña, J. (1996). Aluminium distributions in Central East Atlantic waters (Canary Islands). *Marine Chemistry*, *51*(4), 359–372. doi: 10.1016/0304-

4203(95)00069-0.

Gelado-Caballero, M. D., López-García, P., Prieto, S., Patey, M. D., Collado, C., & Hérnndez-Brito, J. J. (2012). Long-term aerosol measurements in Gran Canaria, Canary Islands: Particle concentration, sources and elemental composition. *Journal of Geophysical Research Atmospheres*, *117*(3). doi: 10.1029/2011JD016646.

Goudie, A. S., & Middleton, N. J. (2001). Saharan dust storms: Nature and consequences. *Earth-Science Reviews*, *56*(1–4), 179–204. doi: 10.1016/S0012-8252(01)00067-8.

Huneeus, N., Schulz, M., Balkanski, Y., Griesfeller, J., Prospero, J., Kinne, S., Bauer, S., Boucher, O., Chin, M., Dentener, F., Diehl, T., Easter, R., Fillmore, D., Ghan, S., Ginoux, P., Grini, A., Horowitz, L., Koch, D., Krol, M. C., Zender, C. S. (2011). Global dust model intercomparison in AeroCom phase i. *Atmospheric Chemistry and Physics*, *11*(15), 7781–7816. doi: 10.5194/acp-11-7781-2011.

Jickells, T. D., An, Z. S., Andersen, K. K., Baker, A. R., Bergametti, C., Brooks, N., Cao, J. J., Boyd, P. W., Duce, R. A., Hunter, K. A., Kawahata, H., Kubilay, N., LaRoche, J., Liss, P. S., Mahowald, N., Prospero, J. M., Ridgwell, A. J., Tegen, I., & Torres, R. (2005). Global iron connections between desert dust, ocean biogeochemistry, and climate. In *Science*, *308*(5718), 67–71. doi: 10.1126/science.1105959.

Jickells, T., & Moore, C. M. (2015). The Importance of Atmospheric Deposition for Ocean Productivity. *Annual Review of Ecology, Evolution, and Systematics*, *46*(1), 481–501. doi: 10.1146/annurev-ecolsys-112414-054118.

Johansen, A. M., Siefert, R. L., & Hoffmann, M. R. (2000). Chemical composition of aerosols collected over the tropical North Atlantic Ocean. *Journal of Geophysical Research Atmospheres*, *105*(D12), 15277–15312. doi: 10.1029/2000JD900024.

Kelly, F. J., & Fussell, J. C. (2015). Air pollution and public health: emerging hazards and improved understanding of risk. *Environmental Geochemistry and Health*, *37*(4), 631–649. doi:10.1007/s10653-015-9720-1.

Korte, L. F., Pausch, F., Trimborn, S., Brussaard, C. P. D., Brummer, G.-J. A., Van Der Does, M., Guerreiro, C. V, Schreuder, L. T., Munday, C. I., & Stuut, J.-B. W. (2018). Effects of dry and wet Saharan dust deposition in the tropical North Atlantic Ocean. *Biogeosciences*, 1–20. doi: 10.5194/bg-2018-484.

Lee, C., Martin, R. V., Van Donkelaar, A., Lee, H., Dickerson, R. R., Hains, J. C., Krotkov, N., Richter, A., Vinnikov, K., & Schwab, J. J. (2011). SO_2 emissions and lifetimes: Estimates from inverse modeling using in situ and global, space-based (SCIAMACHY and OMI) observations. *Journal of Geophysical Research Atmospheres*, *116*(6). doi: 10.1029/2010JD014758.

López-García, P., Gelado-Caballero, M. D., Patey, M. D., Hernandez-Brito, J. J. (2020). *Atmospheric fluxes of soluble nutrients and Fe: more than three years of wet and dry deposition measurements at Gran Canaria (Canary Islands)*. Manuscript under revision.

López-García, P., Gelado-Caballero, M. D., Collado-Sánchez, C., & Hernández-Brito, J. J. (2017). Solubility of aerosol trace elements: Sources and deposition fluxes in the Canary Region. *Atmospheric Environment*, *148*, 167–174. doi: 10.1016/j.atmosenv.2016.10.035.

López-García, P., Gelado-Caballero, M. D., Santana-Castellano, D., Suárez de Tangil, M., Collado-Sánchez, C., & Hernández-Brito, J. J. (2013). A three-year time-series of dust deposition flux measurements in Gran Canaria, Spain: A comparison of wet and dry surface deposition samplers. *Atmospheric Environment*, *79*, 689–694. doi: 10.1016/j.atmosenv.2013.07.044.

Menéndez, I., Derbyshire, E., Engelbrecht, J., Von Suchodoletz, H., Zoeller, L., Dorta

Antequera, P., Carrillo, T & Rodriguez de Castro, F. C. B. (2009). Saharan Dust And The Aerosols On The Canary Islands: Past And Present. *Airborne particulates*, 39-80.

Menédez, I., Díaz-Hernandez, J. L., Mangas, J., Alonso, I. & Sánchez-Soto, P. J. (2007). Airborne dust accumulation and soil development in the North-East sector of Gran Canaria (Canary Islands, Spain). *Journal of Arid Enviroments, 71*, 57-81. doi: 10.1016/j.jaridenv.2007.03.011.

Middleton, J. L., Mukhopadhyay, S., Langmuir, C. H., McManus, J. F., & Huybers, P. J. (2018). Millennial-scale variations in dustiness recorded in Mid-Atlantic sediments from 0 to 70 ka. *Earth and Planetary Science Letters*, *482*, 12–22. doi: 10.1016/j.epsl.2017.10.034.

Millero, F. J. (1974). The Physical Chemistry of Seawater. *Annual Review of Earth and Planetary Sciences*, *2*(1), 101–150. doi: 10.1146/annurev.ea.02.050174.000533.

Morselli, L., Bernardi, E., Vassura, I., Passarini, F., & Tesini, E. (2008). Chemical composition of wet and dry atmospheric depositions in an urban environment: Local, regional and long-range influences. *Journal of Atmospheric Chemistry*, *59*(3), 151–170. doi.org/10.1007/s10874-008-9099-9.

Neuer, S., Torres-Padrón, M. E., Gelado-Caballero, M. D., Rueda, M. J., Hernández-Brito, J., Davenport, R., & Wefer, G. (2004). *Dust deposition pulses to the eastern subtropical North Atlantic gyre: Does ocean's biogeochemistry respond?* doi: 10.1029/2004GB002228.

Pandolfi, M., Amato, F., Reche, C., Alastuey, A., Otjes, R. P., Blom, M. J., & Querol, X. (2012). Summer ammonia measurements in a densely populated Mediterranean city. *Atmospheric Chemistry and Physics*, *12*(16), 7557–7575. doi: 10.5194/acp-12-7557-2012.

Pausata, F. S. R., Gaetani, M., Messori, G., Berg, A., Maia De Souza, D., Sage, R. F., & Demenocal, P. B. (2020). One Earth The Greening of the Sahara: Past Changes and Future Implications. *One Earth*, *2*, 235–250. doi: 10.1016/j.oneear.2020.03.002.

Powell, C. F., Baker, A. R., Jickells, T. D., Bange, H. W., Chance, R. J., & Yodle, C. (2015). *Estimation of the Atmospheric Flux of Nutrients and Trace Metals to the Eastern Tropical North Atlantic Ocean*, *72*(10), 4029-4045. doi: 10.1175/JAS-D-15-0011.s1.

Prospero, J. M. (1999). Long-term measurements of the transport of African mineral dust to the southeastern United States: Implications for regional air quality. *Journal of Geophysical Research Atmospheres*, *104*(D13), 15917–15927. doi: 10.1029/1999JD900072.

Prospero, J. M., Collard, F. X., Molinié, J., & Jeannot, A. (2014). Characterizing the annual cycle of African dust transport to the Caribbean Basin and South America and its impact on the environment and air quality. *Global Biogeochemical Cycles*, *28*(7), 757–773. doi: 10.1002/2013GB004802.

Prospero, J. M., Ginoux, P., Torres, O., Nicholson, S. E., & Gill, T. E. (2002). Environmental characterization of global sources of atmospheric soil dust identified with the Nimbus 7 Total Ozone Mapping Spectrometer (TOMS) absorbing aerosol product. *Reviews of Geophysics*, *40*(1), 2–31. doi: 10.1029/2000RG000095.

Prospero, J. M., & Lamb, P. J. (2003). African Droughts and Dust Transport to the Caribbean: Climate Change Implications. *Science*, *302*(5647), 1024–1027. doi: 10.1126/science.1089915.

Ramanathan, V., Crutzen, P. J., Kiehl, J. T., & Rosenfeld, D. (2001). Atmosphere: Aerosols, climate, and the hydrological cycle. In *Science*, *294*, 2119–2124. doi:

10.1126/science.1064034.

Ridame, C., Dekaezemacker, J., Guieu, C., Bonnet, S., L'Helguen, S., & Malien, F. (2014). Contrasted Saharan dust events in LNLC environments: impact on nutrient dynamics and primary production. *Biogeosciences*, *11*(17), 4783–4800. doi: 10.5194/bg-11-4783-2014.

Rodríguez, S., Cuevas, E., Prospero, J. M., Alastuey, A., Querol, X., López-Solano, J., García, M. I., & Alonso-Pérez, S. (2015). Modulation of Saharan dust export by the North African dipole. *Atmospheric Chemistry and Physics*, *15*(13), 7471–7486. doi: 10.5194/acp-15-7471-2015.

Rodríguez, Sergio, Calzolai, G., Chiari, M., Nava, S., García, M. I., López-Solano, J., Marrero, C., López-Darias, J., Cuevas, E., Alonso-Pérez, S., Prats, N., Amato, F., Lucarelli, F., & Querol, X. (2020). Rapid changes of dust geochemistry in the Saharan Air Layer linked to sources and meteorology. *Atmospheric Environment*, *223*. doi: 10.1016/j.atmosenv.2019.117186.

Rolph, G., Stein, A., & Stunder, B. (2017). Real-time Environmental Applications and Display sYstem: READY. *Environmental Modelling and Software*, *95*, 210–228. doi: 10.1016/j.envsoft.2017.06.025.

Sancho, P., de la Cruz, J., Díaz, A., Martín, F., Hernández, E., Valero, F., & Albarrán, B. (1992). A five-year climatology of back-trajectories from the Izaña baseline station, Tenerife, Canary Islands. *Atmospheric Environment Part A, General Topics*, *26*(6), 1081–1096. doi: 10.1016/0960-1686(92)90040-R.

Seinfeld, J. H. and Pandis, S. N. From air pollution to Climate Change. *Atmospheric Chemestry and Physics, 15*(2), 6219-6234.

Skonieczny, C., Paillou, P., Bory, A., Bayon, G., Biscara, L., Crosta, X., Eynaud, F., Malaizé, B., Revel, M., Aleman, N., Barusseau, J.-P., Vernet, R., Lopez, S., & Grousset, F. (2015). African humid periods triggered the reactivation of a large river system in Western Sahara. *Nature Communications*, *6*, 8751. doi: 10.1038/ncomms9751.

Stein, A. F., Draxler, R. R., Rolph, G. D., Stunder, B. J. B., Cohen, M. D., & Ngan, F. (2015). Noaa's hysplit atmospheric transport and dispersion modeling system. In *Bulletin of the American Meteorological Society*, *96*(12) 2059–2077. doi: 10.1175/BAMS-D-14-00110.1.

Talbot, R. W., Andreae, M. O., Berresheim, H., Jacob, D. J., & Beecher, K. M. (1990). Sources and sinks of formic, acetic, and pyruvic acids over central Amazonia. 2. Wet season. *Journal of Geophysical Research*, *95*(D10), 16799–16811. doi: 10.1029/jd095id10p16799.

Torres-Padrón, M. E., Gelado-Caballero, M. D., Collado-Sánchez, C., Siruela-Matos, V. F., Cardona-Castellano, P. J., & Hernández-Brito, J. J. (2002). Variability of dust inputs to the CANIGO zone. *Deep-Sea Research Part II: Topical Studies in Oceanography*, *49*(17), 3455–3464. doi: 10.1016/S0967-0645(02)00091-7.

Torres, C., Cuevas Agulló, E., Guerra García, J. C., & Carreño Corbella, V. (2001). Caracterización de las masas de aire en la región subtropical. Paper presented at V Simposio Nacional de Predicción, Inst. Nac. de Meteorol., Madrid.

Supplementary materials

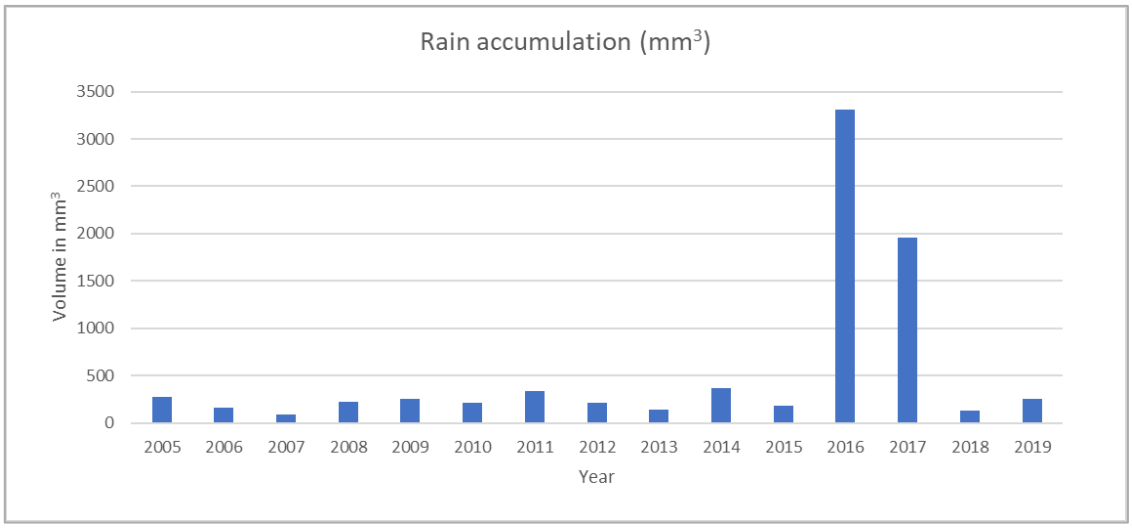

Figure S1: Rain accumulation time series in TF station during 2005-2019.

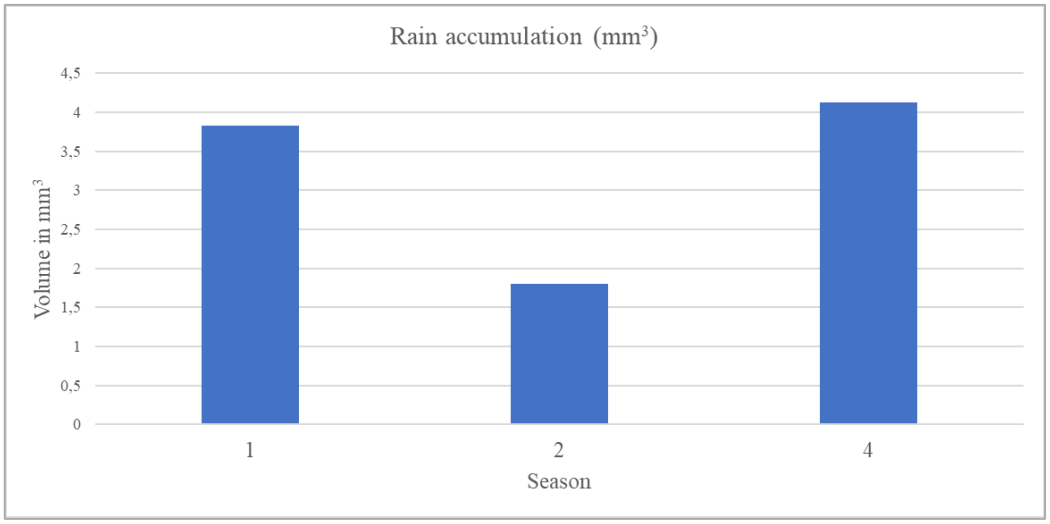

Figure S2: Seasonal rain accumulation during sampling period (January 2018 to March 2020). 1, winter; 2, spring; 4, autumn.

Total flux contribution	**F^-**	**Ac**	**Fo**	**Cl^-**	**Br^-**	**NO_3^-**	**SO_4^{2-}**	**nss-SO_4^{2-}**	**Ox**	**Na**	**NH_4^+**	**K^+**	**Mg^{2+}**	**Ca^{2+}**
%WD	0,04	25,02	8,40	30,25	57,79	4,15	31,72	28,63	1,13	31,38	85,01	24,80	29,94	12,11
%DD	99,96	74,98	91,60	69,75	42,21	95,85	68,28	71,37	98,87	68,62	14,99	75,20	70,06	87,89

Table S1: Contributions of fluxes of soluble elements (%) for DD and WD samples from January 2018 to March 2020. Values for WD represent only the average for raining days. Acid acetic (Ac), Formic (Fo) and Oxalic (Ox).

Memoria final del Trabajo Fin de Grado

Descripción de las actividades desarrolladas durante la realización del TFT

- Recogida y determinación de las fracciones solubles lixiviadas de filtros Whatman de policarbonato y medidas de PH para las muestras de deposiciones secas y húmedas.

- Búsqueda bibliográfica a través de recursos proporcionados por la tutora y en diferentes bases de datos en las que la Biblioteca Universitaria está escrita, como *Web of Science, Scopus, Science Direct o Faro.*

- Tratamiento de datos obtenidos, elaboración de gráficos, elaboración de retrotrayectorias, análisis estadístico y discusión de la información recopilada.

Formación recibida

- HYSPLIT. Software desarrollado por NOA para realizar los mapas de las retrotrayectorias de las masas de aire y determinar el origen tanto el tipo de aerosol.

- Excell. Hoja de cálculo desarrollada por Microsoft para el procesamiento de los resultados obtenidos y representación gráfica.

Nivel de integración e implicación dentro del departamento y relaciones con el personal.

Mi nivel de integración se vio favorecido gracias a la buena actitud de mi tutora, compañeros de laboratorio tanto de los integrantes del Departamento de Química. He tenido la gran suerte de poder trabajar junto a ellos ya que me han hecho sentir uno más del equipo y me han ayudado en todo lo posible, por lo que estoy muy agradecido.

Aspectos positivos y negativos más significativos relacionados con el desarrollo del TFT

Los aspectos más recalcables han sido la satisfacción personal al superar las diferentes adversidades que se dan a lo largo de la realización del TFT, así como la comprensión de los resultados estadísticos obtenidos.

Valoración personal del aprendizaje conseguido a lo largo del TFT

El conocimiento que he adquirido a lo largo de la realización del trabajo me ha permitido ampliar con creces la sabiduría que tenía acerca de los aerosoles atmosféricos, su composición química en relación con su origen, las diferentes reacciones que se pueden producir en la atmósfera, estacionalidades etc., lo que me ha permitido ampliar mi conocimiento en la oceanografía. Además, he fortalecido mi disciplina y constancia necesarias para realizar un TFT y he podido apreciar una parte de todo el trabajo que hay detrás de un trabajo de investigación.